LBL-36028
UC-410
Preprint

Lawrence Berkeley Laboratory
UNIVERSITY OF CALIFORNIA

Accelerator & Fusion Research Division

Submitted to Optical Engineering

Some Fundamentals of Cooled Mirrors for Synchrotron Radiation Beamlines

M. Howells

August 1994

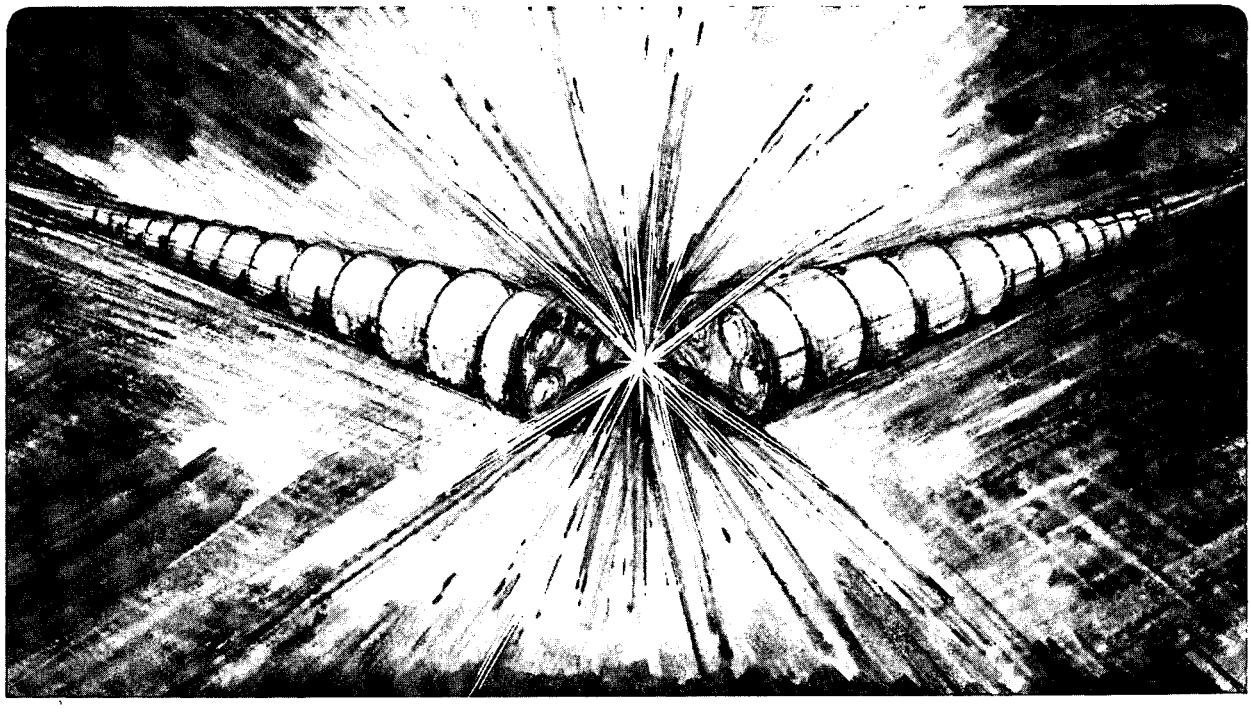

Prepared for the U.S. Department of Energy under Contract Number DE-AC03-76SF00098

DISCLAIMER

LBL-36028
LSGN-185
UC-410

SOME FUNDAMENTALS OF COOLED MIRRORS FOR SYNCHROTRON RADIATION BEAMLINES*

M. Howells

Advanced Light Source
Accelerator and Fusion Research Division
Lawrence Berkeley Laboratory
University of California
Berkeley, CA 94720

August 1994

Paper invited by Optical Engineering

*This work was supported by the Director, Office of Energy Research, Office of Basic Energy Sciences, Materials Sciences Division, of the U.S. Department of Energy, under Contract No. DE-AC03-76SF00098.

SOME FUNDAMENTALS OF COOLED MIRRORS FOR SYNCHROTRON RADIATION BEAM LINES

M. R. Howells

The Advanced Light Source, Lawrence Berkeley Laboratory, Berkeley, CA 94720 USA

Abstract

We give an analysis using conventional heat-transfer theory of a common type of cooled beam-line mirror with rectangular cooling channels. The analysis leads to a simple analytic expression for the slope error which allows the distortion performance to be estimated in practical situations thus providing a way to develop designs. It also provides understanding of the effect of the various parameters on the goodness of the cooling process and some insight into the underlying physics. The analysis is applied to the question of comparing the thermal properties of candidate mirror materials with respect to slope-error performance in an example mirror design. The best performance was obtained from (in order) invar, silicon carbide and silicon.

Keywords

High-power optics, x-ray mirrors, synchrotron-bream-line optics, water cooling.

Introduction

The design of cooled mirrors for synchrotron radiation beamlines has already acquired a substantial literature including a number of reviews[1] workshop reports[2, 3] and conference proceedings[4, 5] dedicated to the subject. There are now many reports on the record of successful mirror designs developed to withstand particular heat loads with given surface accuracy tolerances. Usually such reports rely on commercially-produced finite-element codes to verify that the design meets its requirements and this appears to be a perfectly sound approach reflecting the basic validity of classical heat-transfer theory in cases of interest to the synchrotron radiation community.

Although the use of finite element codes is an essential part of mirror engineering it has one unwelcome feature that is shared with many computer-aided design proceedures. This is the loss of some of the insight and intuition which accompanies the more traditional analytical approaches. Some writers have begun to address this by investigating the general effect of the various design parameters on the ultimate surface accuracy of the mirror[1, 2, 6, 7] and there appears to be a need for more studies of this type.

In this study we give an analytic treatment of a common type of cooled beam-line mirror using conventional heat-transfer theory. Although the model is quite specific, it illustrates well the effect of the most important design parameters and provides insight into the underlying physics. It also gives a starting point for consideration of material choices and some guidance in the process of developing candidate mirror designs which is a step that must always precede the finite element calculations.

Basic ideas of distortion and cooling

Gross bending of the whole mirror

Suppose initially that we have a simple unconstrained rectangular block with the top held at a temperature ΔT greater than the bottom. The top surface would become longer by $L\alpha\Delta T$ (strain=$\alpha\Delta T$), and the block would bend into a radius $t/\alpha\Delta T$ where α is the coefficient of linear expansion of the mirror, L its length and t its thickness. If the block were constrained not to expand in the longitudinal direction, then the stress would be $Y\alpha\Delta T$ where Y is the Young's modulus of the mirror material. This gives us an order of magnitude for the stresses to expect when expansion is prevented, and provides a primary reason why low values of ΔT are very desirable, even if they are not mandated by distortion considerations.

Although such a gross-bending effect is a well-known potential problem in designing cooled mirrors, it is relatively easy to prevent. It is predictably associated with back-cooling schemes and these should therefore be avoided. For an undulator, only a small fraction of the top area is illuminated, which tends to make the gross bending effect small. Even for bending magnets and wigglers, where larger areas can be illuminated, it is still straightforward to counter the tendancy to gross bending by the cooling and stiffening strategies described below which are in regular use by the community.

The mapping distortion

Since the gross bending effect is easy to avoid, we concentrate attention in what follows on the so-called "mapping distortion" which is more difficult to control. This is the local swelling due to direct expansion of the heated material normal to the heated surface which leads to a distortion which "maps" the power density distribution. Although, in the most general case, the gross-bending and mapping distortions are not seperate effects, the distinction is, nonetheless, helpful in thinking about many of the most common geometries of real synchrotron-radiation mirrors. We will calculate the mapping distortion of a mirror illuminated with a slowly varying power density distribution such as an unapertured beam from a bending magnet or a wiggler. The fact that the power density is always rapidly varying at the edge of the beam can be overcome by placing the edge outside the clear aperture of the system.

General principles of cooling

The natural way to address the problem of a high incoming heat load on a mirror is to provide cooling channels just under the surface. Such channels should evidently be as close as possible to the heated surface consistent with enough mechanical strength to resist the forces due to polishing and water pressure. Practical wall thicknesses are normally in the range 0.5-5 mm. This general situation is represented in Fig. 1 which also shows the notation to be used. There is a thin (and therefore flexible) layer of material above the water channels known as the "hot wall", which has a temperature gradient across it and which, if unrestrained, would develop a convex curvature. Underneath the water channels is a large thick block; the main mirror substrate, which should have a much greater stiffness (thickness) than the hot wall. The latter is therefore prevented from expanding or bending and develops compressive stresses at its top surface. The purpose of the design is to remove all the incoming heat via the water which implies that the whole lower substrate should be at a uniform temperature equal to that of the water.

The heat flow will be from the top surface to the water with a conductive temperature drop across the hot wall and a convective temperature drop across the solid-water interface. Following normal practice in heat transfer we consider that these are determined by a conductivity, k, and a convective heat transfer coefficient, h, defined generically as follows

$$\dot{Q}'' = k\frac{\Delta T}{\Delta x} \quad \text{and} \quad \dot{Q}'' = h\Delta T \tag{1}$$

where $\dot{Q}''(y,z)$ is the deposited power density, the ΔT's in our case are the temperature differences $T_M - T_0$ and $T_0 - T_W$ (in Fig. 1) respectively and T_W is the bulk (free-stream) water temperature which we take, without loss of generality, to be zero. Making an analogy between the the flow of heat in these cases and an electric current, one can define a thermal "resistance" $\theta = \Delta T / \dot{Q}''(y,z)$ which in our problem has two parts in series: $\theta = \theta_k + \theta_h$. We know that when we turn on the heat flow through θ_k and θ_h, T_M and T_0 will increase from their initial values of zero and there will be an expansion of the mirror material and an increase, x, in the height of the surface. If $\dot{Q}''(y,z)$ is nonuniform, there will also be nonzero values for $\partial x/\partial y$ and $\partial x/\partial z$ which are the slope errors we wish to calculate and eventually minimize.

To make a quantitative analysis we need to assume a shape for the cooling channels and we choose the rectangular one shown in Fig. 2 which easy to manufacture, close to optimum in performance and amenable to calculation. We are thus assuming that the channels are of *uniform cross section.* This excludes for the moment such schemes as the cellular-pin-post design but our treatment will provide insight into that system and we will return to it later. We are now in a position to summarize the features of the model we are trying to analyze:

- attention limited to the mapping distortion
- $\dot{Q}''(y,z)$ slowly varying compared to the size of the cooling channels
- rectangular cooling channels of uniform crossection
- neglect of effects due to the heating of the water.

Cooling by rectangular fins

Theory of rectangular fins

We consider the rectangular segments of mirror material between the water channels in Fig. 2 to be "cooling fins" for the hot wall. The properties of such structures have long been analysed in the engineering literature[8,9]. For suitably good conductors, a fin can remove much more power per unit area per unit temperature difference (relative to the water) than can a direct solid-water interface. To verify this statement quantitatively consider fins of width w, height H and length L ($>>w$) as shown in Fig. 2. Suppose that the power flux and temperature are P_0 and T_0 at the base of the fin and P and T at a distance p from the base. We make the assumptions normally used in analyzing fins: (i) that the heat flow is one-dimensional down the fin and (ii) that the heat transfer coefficient h is uniform over the area of the fin and argue as follows. The power transfered to the water between p and $p+dp$ is given by $-dP = 2hTLdp$ and that flowing through dp is given by $P = -kLw\, dT/dp$. Taking the derivative of the latter relation we find the differential equation of the problem

$$\frac{d^2T}{dp^2} - \frac{2h}{kw}T = 0. \tag{2}$$

The solution of this equation is $T = Ae^{mp} + Be^{-mp}$ where $m^2 = 2h/kw$. The boundary condition at the base of the fin is determined by the need to remove a prescribed amount of power per unit area based on the

incoming power density. The boundary condition at the end of the fin comes from the assumed philosophy for designing the fins which is to make their height (H) great enough so that all the power is transfered through their sides and none through their bottom ends. We thus write for the boundary conditions

$$\left[\frac{dT}{dp}\right]_{p=0} = \frac{-P_0}{kLw} \quad \text{and} \quad \left[\frac{dT}{dp}\right]_{p=H} = 0. \tag{3}$$

Applying these leads to the formal solution to our problem;

$$T(p) = \frac{P_0}{Lw}\frac{1}{km}\frac{\cosh[m(H-p)]}{\sinh(mH)} \tag{4}$$

Choice of fin parameters

Equation (4) enables one to calculate the temperature rise, $T(0)$ at $p=0$ due to removal of the given amount of power in terms of quantities that are known or can be chosen. To choose H we note that for $p=0$ the last term of equation (4) is equal to $\coth(mH)$ which approaches its lowest value of unity as H becomes large. We would like to achieve this lowest value and to get within 10% of it we only need to have $mH \geq 1.522$. With this in mind we can use equation (4) for $p=0$ to determine the thermal resistance of unit area of the fin base

$$\theta_{fin} = \frac{T(0)}{P_0/Lw} = \frac{1}{km^2H}\left[\frac{mH}{\tanh(mH)}\right]. \tag{5}$$

The quantity in square brackets is the reciprocal of the so-called "fin efficiency factor" (η_f). This quantity is defined in texts on heat transfer (using slightly different boundary conditions than ours)[9] as the actual heat transfered by the fin divided by the heat that would have been transfered if the entire fin had been at base temperature. We now have

$$\theta_{fin} = \frac{w}{2hH\eta_f}. \tag{6}$$

Conduction- and convection-limited heat flow

We can recast (6) in a way that provides a better understanding of the role of the conductivity

$$\theta_{fin} = \frac{1}{hR\eta_f}, \tag{7}$$

where R is approximately the ratio of the area of the solid-water interface to the area illuminated. This tells us that apart from the fin efficiency factor, the convective thermal resistance is *the same as if we had assumed infinite conductivity and used* $\dot{Q}'' = h\Delta T$ *alone*. If the conductivity is good enough one reaches a condition where the heat flow is dominated by the convective thermal resistance, and the conductivity has

only a weak effect (through η_f). When the convective thermal resistance is important, the traditional way to achieve a low value for it, is therefore to make H large enough to have $\coth(mH)$ near unity, w and c small enough to make $R>>1$ (ie use a high number of high-aspect-ratio channels) and h large by means of turbulent flow conditions.

We now derive the full expression for the temperature rise at the base of the fin. Up to now we have not included the heat transfered directly through the tops of the channels which is not negligible in the case of a low conductivity mirror. If the fins occupy a fraction F of the total area then the overall convective thermal resistance θ_h is given by $1/\theta_h = F/\theta_{fin}+(1-F)/\theta_{ch}$. Going back to (6) for θ_{fin} and using $\theta_{ch}=1/h$ we find that

$$\theta_h = \frac{1}{h\left[\frac{2FH\eta_f}{w}+1-F\right]} \tag{8}$$

This gives us the useful quantity, T_0, which is an average temperature in the plane $x=-t$.

$$T_0 = \dot{Q}''\theta_h \tag{9}$$

We now make the assumption that the temperature of the mirror material in the plane $x=-t$ is approximately uniform and equal to T_0 (Fig. 1) so that, bearing in mind that $\dot{Q}''$ is slowly varying, we can treat the hot wall as undergoing linear heat flow which means that its temperature drop is given by

$$\Delta T_{0M} = \dot{Q}''t/k. \tag{10}$$

The last two equations show that the temperature rise at the surface maps $\dot{Q}''$. It also follows that the conductive thermal resistance is given by.

$$\theta_k = t/k. \tag{11}$$

The dominant thermal resistance is likely to be θ_k for materials of low conductivity and θ_h for materials of high conductivity. The heat flow can therefore be classified as either conduction-limited (poor conductor, θ_k dominant) or convection-limited (good conductor, θ_h dominant). We are now in a position to evaluate θ_k and θ_h provided we know how to calculate h which is the subject of the next section.

Analysis of convective heat transfer

Calculation of the convective heat transfer coefficient

The estimation of h in practical situations is thoroughly discussed in standard texts on heat transfer[9] and we will quote the needed results here. For fully developed turbulent flow in a smooth tube, far from the tube entrance and under constant-heat-flow conditions, the following empirical relation is recommended[10].

$$Nu = 0.027(Re)^{0.8}(Pr)^{1/3}. \tag{12}$$

The quantities *Nu, Re* and *Pr* are dimensionless numbers defined below and are to be evaluated at the free stream water temperature.

$Nu = \frac{hD_h}{k_w}$: *Nu* is the Nusselt number, k_w is the thermal conductivity of the water while D_h is the hydraulic diameter (four times the area divided by the perimeter).

$Re = \frac{\rho v D_h}{\mu}$: *Re* is the Reynolds number, ρ is the density, v the free stream velocity and μ the fluid dynamic viscosity. For turbulent flow, $Re>2300$, for laminar flow, $Re<2000$.

$Pr = \frac{\mu c_p}{k_w}$: *Pr* is the Prandl number, c_p is the specific heat at constant pressure. The above relation (12) is valid for $0.6<Pr<100$.

Equation (12) is simple but subject to errors of up to 25% in extreme cases. A more accurate but more complicated formula is given by Petukhov[10] which is also free of the limitation to smooth tubes.

For laminar flow in a sufficiently long circular tube, *Nu* approaches the constant value 3.66. Laminar flow is sometimes of interest in mirror design because of "quietness" considerations but it provides inferior net heat transfer compared to turbulent flow unless one has very many channels of microscopic width and very small length. For a more complete treatment of noncircular, short tubes the reader is referred to the standard texts such as Holman[9]. A tabulation of the quantities needed to calculate *h* for water from equation (12) is given in the Appendix.

A reference design of a water-cooled mirror

As an example, consider a mirror with the geometry given in Table 1, cooled with 20°C water with a flow velocity of 3m/sec[11]. We will use this as a reference design and for the moment we take it to be made from the copper alloy Glidcop (see Table 2 for a list of material properties). The power density is that of one of the wigglers at the European Synchrotron Radiation Facility. These parameters lead to D_h=1.71mm, *Re*=5132 (turbulent flow), *Nu*=47.9 and finally h=0.017 W/mm^2/°C.

Table 1. Reference mirror design parameters

Parameter	Symbol	Value
Hot wall thickness (mm)	t	2.0
Channel width (mm)	c	1.0
Fin width (mm)	w	1.0
Fin height (mm)	H	6.0
Water velocity (m/sec)	v	3.0
Peak input power density (W/mm^2)	$\dot{Q}''(0,0)$	0.46
Storage ring energy (GeV)	E	6
Grazing angle (°)	α	1

Source-mirror distance (m)	r	30
Rms width of beam footprint (mm)	σ_y	77.6
Plane of reflection		vertical

Returning now to equation (8) with p=0 we find that the coth term is indeed close to 1 and therefore the heat removed by the fin per unit area, per unit temperature rise is approximately km. This is to be compared with the corresponding figure for a direct solid-water interface which, by definition, is h. The fin thus removes $km/h=(2k/hw)^{1/2}$ (=6.6 for the reference design) times more heat per unit area per unit temperature difference than the direct interface. This fin advantage factor becomes even larger for smaller channels roughly as $w^{-1/2}$ because h is almost independant of D_h. However, for poor conductors and wide fins, the fin advantage becomes smaller and may turn into a disadvantage. We note however, that at least some fins are always needed for structural reasons.

Calculation of thermal distortions

Alteration of the expansion of material due to partial restraint

Before we estimate the distortion we have to account for the effect of the specific restraints which are applied to the heated regions of the mirror. We assume that the hot wall is restrained in two dimensions, the length and width directions of the mirror, and is unrestrained in the thickness direction while the fins are restrained in only one dimension, the length. The application of the known relationships between the stresses, strains and moduli of an isotropic material then tells us that the strain is $(1+\nu)/(1-\nu)$ times as large for two-dimensional restraint and $(1+\nu)$ times as large for one-dimensional restraint than it would be in the absence of restraint where ν is Poisson's ratio. Since the strain is $\alpha\Delta T$ for an unrestained block of heated material, the difference can be accounted for by defining two new expansion coefficients α_1 and α_2

$$\alpha_1 = \alpha(1+\nu) \quad \text{and} \quad \alpha_2 = \alpha\left(\frac{1+\nu}{1-\nu}\right). \tag{13}$$

Expansion of the hot wall

The temperature, $T(x)$ in the hot wall is given by $T_0+\Delta T_{0M}(1+x/t)$ and for each element dx the growth of the wall thickness compared to zero temperature is $\alpha_2 T(x)dx$. The overall growth, x_{wall}, is thus

$$x_{wall} = \alpha_2 \int_{-t}^{0} T(x)dx = \alpha_2 \dot{Q}'' t\left[\theta_h + \frac{\theta_k}{2}\right]. \tag{14}$$

where we have used equations (9), (10) and (11).

Expansion of the fins

The temperature $T(x)$ in the fin is given by equation (4) so we find similarly

$$x_{fin} = \alpha_1 \int_{-H-t}^{-t} T(p)dp = \frac{\alpha_1 P_0}{Lwkm\sinh(mH)} \int_0^H \cosh(m(H-p)dp$$
$$= \frac{\alpha_1 P_0}{Lwkm^2} = \dot{Q}''\alpha_1 h\eta_f \theta_h \tag{15}$$

where we have used equations (5), (6) and (9).

Calculation of mirror surface slope errors

We can now proceed to evaluate the total growth, x, in the thickness of the mirror which can be expressed in terms of the thermal resistances using (14) and (15) as follows

$$x = \dot{Q}''\left\{\alpha_1 H\eta_f\theta_h + \alpha_2\theta_h t + \frac{\alpha_2\theta_k t}{2}\right\}. \tag{16}$$

Expressing this in terms of design parameters and making the y and z dependences explicit we finally arrive at

$$x(y,z) = \dot{Q}''(y,z)\left\{\frac{\frac{\alpha_1}{h}H\eta_f + \frac{\alpha_2}{h}t}{\frac{2FH\eta_f}{w} + 1 - F} + \frac{\alpha_2}{k}\frac{t^2}{2}\right\}. \tag{17}$$

Equation (17) represents our approximate analysis of the thermal distortion of the mirror. We may summarize it as $x = A\dot{Q}''$ or $\partial x/\partial y = A\partial(\dot{Q}'')/\partial y$ etc in which case the quantity A, the height error per unit power density is a measure of the goodness of the cooling and is known in some communities as the "worm factor". The first term in the curved brackets describes the growth in the length of the fins while the second and third terms both represent a growth in thickness of the hot wall. The second term describes the growth due to the rise in the temperature of the fin-hot-wall interface consequent on the convective heat transfer. The third term describes the growth due to the conductive top-to-bottom temperature difference (ΔT_{0M}) across the hot wall. From equation (16) one can see that the θ_h terms will dominate for convection-limited heat flow and the θ_k term for conduction limited heat flow.

The significance of the so-called "distortion figure of merit" k/α becomes clearer. It determines the growth of the hot wall thickness due to ΔT_{0M} which is the main effect when the mirror is made from low conductivity material leading to conduction-limited heat flow. On the other hand the importance of h/α in determining the size of the first two terms which dominate for high conductivity mirrors with convection-limited heat flow is also evident. Thus k/α is not a true, simple figure of merit in this situation. In our reference design, for example, the last term, which contains k/α, represents only about one tenth of the total distortion.

Another feature of equation (17) is that the growth, x, in the surface height depends on position only through the position dependance of the incoming power density $\dot{Q}''$ so that our calculated height error is indeed the expected "mapping" of the input power density distribution. Thus we expect *the maximum slope errors at regions of maximum spatial rate of change of the incoming power density* $\dot{Q}''$. The dependance of the slope on t is in accord with intuition: the thinner the hot wall, the less material there is to expand and the smaller is the ΔT_{OM} available to expand it. A thin hot wall is also indicated by the need to avoid gross bending and minimize stress. The choices of the other parameters (small w and c, large R, large h) mentioned earlier are all reafirmed.

Application of the analysis to the reference design.

In order to apply this treatment to a real case we need to know the form of $\dot{Q}''$ for which we use the gaussian approximation. This leads to

$$x(y,z) = A\dot{Q}''(0,0)\exp\left[-\frac{y^2}{2\sigma_y{}^2}\right] \qquad \sigma_y \cong \frac{0.530r}{\gamma \sin\alpha} \tag{18}$$

where $x(0,0) = A\dot{Q}''(0,0)$ and the other notation is given in Table 1. This equation allows the values for x, $\partial x/\partial y$ and $\partial^2 x/\partial y^2$, representing the errors in the height, slope and curvature of the mirror relative to the unheated shape, to be easily calculated. For example the longitudinal radius of curvature at (0,0), $R_y = \left(\partial^2 x/\partial y^2\right)^{-1} = \sigma_y^2/x(0,0)$.

Applying the foregoing equations to the reference design using the values in Table 1, we find, $x(0,0)$= 1.34 μm, T_0=7.5 °C, T_M=10.0 °C and that θ_h is about three times as large as θ_k. The longitudinal radius of curvature would be 4.5 km, and the maximum slope error (at $y=\sigma_y$), 10 μradians.

By neglecting all but the first two terms of the gaussian in equation (18) one can see that, over a certain region near the axis ($y<<\sigma_y$), the thermal swellings are approximately circular. In this region they are therefore correctable by radius tuning. This would apply, for example, within the central cone of an undulator beam so that, in that case, the correction would normally be good over the whole mirror.

Comparison of the calculated performance of the reference design for various materials

Although our treatment has been approximate, it highlights a number of systematic effects which are involved in formulating mirror designs and choosing materials. We now consider the reference design using a wide range of possible materials to make the systematics clearer. Firstly we show in Fig. 3 the variation of the conductive and convective thermal resistances in the reference design with the thermal "resistivity" (k^{-1}) of the mirror material. As expected the thermal resistance curves have a crossover. The graph shows that the dominant thermal resistance is the convective one on the high conductivity (convection-limited heat flow) side of the crossover and conversly on the other side. Fig. 3 also shows the mirror surface temperature which is seen to increase monotonically with decreasing conductivity. This is an important consideration because it can rule out some otherwise interesting materials, such as low expansion glasses. It also reminds us that, for some materials, the expansion coefficient increases considerably with temperature which gives yet another reason why high surface temperatures are undesirable. This applies with particuler force to ULE, invar and superinvar whose low expansion properties apply over quite narrow temperature ranges (see footnotes to Table 2). On the other hand we

should point out that a reasonably high surface temperature is said to be beneficial in preventing contamination of the surface by hydrocarbons.

A primary purpose of mirror cooling is to achieve a sufficiently low slope error. In Fig. 4 we show the value of the *maximum (peak-to-valley)* slope errors for our example mirror and heat load for nine candidate materials. We see that, in spite of the relatively high heat load, the majority of the materials give errors that would be within tolerance for many applications, showing that our reference design is quite useful. It is noteworthy that if the materials were placed in order of slope errors, they would be, with few exceptions, in *inverse order* of ease of fabrication and general convienience. The relative slope errors of the materials in Fig. 4 provide a reasonable comparison of the goodness of the *thermal properties* of the materials for achieving low slope errors. In particular it is a more meaningful comparison than one would get by simply using the k/α values. On the other hand Fig. 4 does not address the temperature rise nor the other issues of fabricability, cost, polishability, dimensional stability, vacuum compatibility etc that are involved in engineering a real mirror.

Improvements to the reference design: narrower fins

Considering a single design for all of the materials is revealing in certain ways but it is not realistic. For conduction-limited cases it is less important to have good fin design, in fact the fin advantage tends to dissapear in such cases, but it is very important to have a thin hot wall both for better slope errors and lower temperatures. To the extent that the lower conductivity materials are useful, this is the key to using them. To have a thin hot wall it is also necessary to keep the channel width small enough compared to the hot wall thickness to avoid "print through" of the underlying structures and one can certainly go smaller than the 1-mm channels and 2-mm wall in the reference design. For materials like steel it should be quite practical to use 0.5-1 mm hot walls with appropriate care. On the other hand for convection-limited cases the hot-wall thickness is less important than good fin design. This also means narrow fins and channels, the limit being set in this case by the need to maintain turbulent flow. To illustrate the effect of pushing the sizes of the fins, channels and hot-wall closer to the limit, we show in Fig. 4 an "improved" design for which the fins and channels are both 0.5×3 mm^2 and the hot wall is 1 mm thick. This leads to the marginal value of 2566 for the Reynold's number. By evaluating the friction factor[9] one can determine that the pressure drop involved in feeding water through such a structure is 0.24 MPa (35 psi) per meter of mirror length as opposed to 0.10 MPa (15 psi) per meter for the original reference design. It is noteworthy that the effect of reducing the hot wall thickness is especially significant for invar because it reduces the mirror surface temperature which reduces the expansion coefficient in addition to the other effects.

Much narrower fins and channels have been used by Tuckerman[12]. The work of this author on the cooling of silicon chips has shown that one can get very effective cooling with fins and channels on the order of 50 μm wide microfabricated in silicon. This moves the design into the laminar flow regime with a correspondingly reduced flow rate while the water temperature rise and pressure drop become substantial. The Tuckerman designs live with this and gain some advantage in h value by using sufficiently *short* flow distances. Heat transfer coefficients greater than 0.1 $W/mm^2/°C$ were achieved for nominal 1-cm flow paths. The same concept has been applied by Arthur and coworkers[13] to cooling x-ray monochromator crystals and a similar h value was achieved. However, microchannels are much less appropriate for cooling large objects like grazing-incidence mirrors. For comparison the overall h values achieved by the reference design are about 0.045 $W/mm^2/°C$ for the Glidcop mirror and lower for the others in inverse proportion to the temperature rise. Much higher overall h values can be achieved using the cellular-pin-post scheme which is described below.

The cellular-pin-post cooling geometry

Silicon has been a somewhat neglected material for beamline optics in view of its excellent properties. It is rather difficult to find reports of the use of silicon for making grazing-incidence mirrors, which is due in part to classification. The favorable thermal and engineering properties of silicon have been exploited by the group at Rockwell[14], which has produced a series of silicon mirrors cooled by water in the so-called "cellular-pin-post" geometry which is explained in Fig. 5. The construction[15, 16] consists of several silicon plates which are machined by conventional ultrasonic techniques and bonded together by means of melted glass ("frit" bonding). The design produces a rapid turbulent flow at the underside of the hot wall and heat transfer is by both the pin fins and the rectangular fins as well as directly to the underside of the wall. This is by far the highest performance scheme for water cooling of mirrors that we know of. A particularly strong feature is the flow geometry in which the water channels are narrow in the region where the coolant interacts with the hot wall and much wider elsewhere. The effect is that for realistic pressures the coolant flow speed *at the hot wall* is as much as an order of magnitude higher than the values one can achieve with channels of uniform crossection. Equation 12 shows that this strategy should yield an almost linear improvement in heat transfer coefficient with coolant velocity and this is indeed realized with overall heat transfer coefficients greater than 1.0 W/mm^2/°C having been achieved. The low surface temperatures that go with such a high h value coupled with the excellent thermal properties of silicon, lead to an outstanding slope-error performance.

Conclusion

We have presented an analysis of a simple but common type of high-power mirror design employing rectangular cooling channels. An analytic expression is obtained representing the predicted height and slope errors of the mirror surface in terms of the parameters of the cooling geometry and heat-load. This allows an understanding of how to choose the design parameters in the best way and gives a considerable degree of insight into the physics of the cooling process. The analytic expression was applied to the question of comparing the thermal properties of candidate mirror substrate materials with respect to the slope errors that they would deliver using an example mirror design. The best performance was obtained from (in order) invar, CVD silicon carbide and silicon.

Acknowledgements

The author is happy to acknowledge helpful conversations with N. Andresen, F. Anthony and C. Corradi. It is also a pleasure to acknowledge the help of R. Avery who read the manuscript in detail, discovered errors and suggested significant improvements. This work was supported by the United States Department of Energy under Contract Number DE-AC03-76SF00098.

APPENDIX: Material properties data on water and candidate mirror materials.

The thermal and elastic properties of a number of candidate mirror materials are listed in Table 2. The sources of the data are indicated in the footnotes. It often happens that there are conflicting values in the literature and a certain amount of judgement has to be used. This can be avoided to some extent by using data compilations such as those of Touloukian [17-20], Barnes[21] and Killpatrick[22-24] where such judgement has already been excercised. Tabulating the properties of silicon carbide presents particular difficulties because the literature contains a wide spread of values for some of the quantities. For the CVD material, the k and α values are selected either because they are recent measurements on optical grade material or are recommended values from data compilations. Electroless nickel and borosilicate glass present similar problems in choosing a single representative number for what is essentially a family of materials. However since these materials tend to be less important in heat transfer calculations we provide only average values.

The properties of water[25] needed for calculating the heat transfer coeficient h are given in Table 3 for $0 \le T \le 100°C$.

Table 2 Room Temperature Elastic and Thermal Properties of Candidate Mirror Materials.

Material	Young's Modulus (10^{10} N/m^2)	Poisson's ratio (v)	Density (10^3 kg/m^3)	Thermal expansion coefficient α, (10^{-6}/°C)[19, 20]	Thermal conductivity (k) (W/m/°C)[17, 18]	k/α (10^6W/m)	Specific heat (J/kg/°C)
Fused silica[26]	7.32	0.167[21]	2.20	**0.49**	1.38	2.8	741[21]
ULE[27]	6.76	0.17	2.21	0±0.03*	1.31	>43.7	766[21]
Borosilicate glass[28].	6.2	0.20	2.2	**3.1**	**1.23**	0.40	710
Silicon (intrinsic)[24]	16.3	.22	2.33	**2.6**	**148**	56.9	750
Silicon carbide:							
CVD[29]	46.5	0.21	3.21	2.4, 3.3	200, 144, 160, 90[30, 31]	52.5**	733
Reaction bonded[24]	22.9	0.14	2.92	2.5	152	60.3	670
Aluminum:							
6061-T6[24]	7.00	0.33	2.78	**23.1**	**237**	10.2	917
Alloy SXA[32]	14.5	0.33	2.96	10.8	217	20.1	960
Beryllium[24]	30.4	0.04	1.85	**11.3**	**200**	17.7	1820
Copper:							
OFHC[21]	11.7	0.33	8.94	**16.5**	**398**	24.1	385
Glidcop (AL-15)[33]	10.3	0.33	8.84	16.6	365	22.0	-
Invar[34]	14.5	0.259	8.08	**0.15*****	**13.8**	106.1	460[9]
Molybdenum[21]	31.4	0.32	10.20	**4.8**	**138**	28.8	251[9]
Electroless nickel, 11% P[24]	11.0	0.41	8.00	12.5	7.4	0.60	460
Stainless steel 304[28]	19.6[34].	0.30[34].	7.94	**14.7**	**15.2**	1.03	502

Table Notes:

The source of data is normally indicated in the left column, however, for authoritative "recommended values", the values are shown in bold type and the source is given at the top of the column. Exceptions are marked individually. For Glidcop, ULE

and SXA, the indicated manufacturer's data is mostly used. Figures for borosilicate glass and electroless nickel are subject to variations of about ±10% for the range of compositions commonly found.

*For $5<T°C<35$

**Based on averages of the quoted α and k value

***$-0.02<\alpha<0.4$ for $0<T°C<80$ according to[19]

Table 3. Quantities needed to calculate the heat transfer coefficient (h) for water*

Temp (°C)	Density (gm/cc)	Specific heat at constant pressure (J/gm/°C)	Thermal conductivity (W/m/°C)	Fluid-dynamic viscosity (gm/m/s)	Prandl number
00	1.0000	4.217	0.569	1.755	13.02
10	1.0000	4.193	0.587	1.301	9.29
20	1.0000	4.182	0.603	1.002	6.95
30	1.0000	4.179	0.618	0.797	5.39
40	0.9901	4.179	0.632	0.651	4.31
50	0.9901	4.181	0.643	0.544	3.53
60	0.9803	4.185	0.653	0.462	2.96
70	0.9803	4.190	0.662	0.400	2.53
80	0.9708	4.197	0.670	0.350	2.19
90	0.9615	4.205	0.676	0.311	1.93
100	0.9615	4.216	0.681	0.278	1.273

*Note that these quantities are given in common units but not in a compatible set for forming the dimensionless numbers.

References

1. R. T. Avery, "Thermal Problems on High Flux Beamlines", *Nucl. Instrum. Meth.*, **222**, 146-158 (1984).
2. R. Smither, "Summary of a Workshop on High Heat Load X-ray Optics Held at Argonne National Laboratory", *Nucl. Instrum. Meth.*, **A291**, 286-299 (1990).
3. A. K. Freund, "Summary of the Satellite Workshop on Thermal Properties of Synchrotron Radiation Optics", *Rev. Sci. Inst.*, **63**, 1623-4 (1992B).
4. A. M. Khounsary, (Ed.) "*High Heat Flux Engineering II*", Proc.SPIE, vol. 1997 (SPIE, Bellingham, 1993).
5. A. M. Khounsary, (Ed.) "*High Heat Flux Engineering*", Proc. SPIE, vol. 1739 (SPIE, Bellingham, 1992).
6. A. K. Freund, F. d. Bergevin, G. Marot, C. Riekel, J. Susini, L. Zhang, E. Ziegler, "X-ray Mirrors for the European Synchrotron Radiation Facility", *Opt. Eng.*, **29**, 928-941 (1990).
7. R. DiGennaro, W. R. Edwards, E. Hoyer, "Predicting Thermal Distortion of Synchrotron Radiation Mirrors with Finite Element Analysis" in *Insertion Devices for Synchrotron Sources,* R. Tatchyn, I. Lindau, (Eds.), Proc. SPIE., vol. 582, 273-280, (SPIE, Bellingham, 1985).
8. M. Jakob, *Heat Transfer*, vol. I, (John Wiley, New York, 1949).
9. J. P. Holman, *Heat Transfer, 6th edition*, (McGraw-Hill, New York, 1986).
10. B. S. Petukhov, "Heat Transfer and Friction in Turbulent Pipe Flow with Variable Physical Properties" in *Advances in Heat Transfer*vol. 6, 504-564, (Academic Press, New York, 1970).
11. R. DiGennaro, T. Swain, "Engineering for High Heat Loads on ALS Beamlines", *Nucl. Inst. Meth.*, **A291**, 313-6 (1990A).
12. D. B. Tuckerman, PhD thesis, Stanford (1984).
13. J. W. Arthur, H. Thompkins, C. Troxel, R. J. Contolini, E. Schmitt, D. H. Bilderback, C. Henderson, J. White, T. Settersten, "Microchannel Water Cooling of Silicon X-ray Monochromator Systems", *Rev. Sci. Inst.*, **63**, 433-7 (1992).

14. Rockwell Power Systems, 2511C, Broadbent Avenue Parkway NE, Albuquerque, NM 87107, USA.

15. T. W. Tonnessen, J. Arthur, "Cooled silicon crystal monochromator test results" in *High Heat Flux Engineering,* A. Khounsary, (Ed.) Proc. SPIE, vol. 1739, 622-627, (SPIE, Bellingham, 1992A).

16. T. W. Tonnessen, S. E. Fisher, "Design and Analysis of cooled optical components for synchrotron beamlines" in *Optics for High-Brightness Synchrotron Radiation Beamlines,* J. Arthur, (Ed.) Proc. SPIE, vol. 1740, 18-23, (SPIE, Bellingham, 1992B).

17. Y. S. Touloukian, R. W. Powell, C. Y. Ho, P. G. Klemens, *Thermal Conductivity Metallic Elements and Alloys,* Thermophysical Properties of Matter, vol. 1, (IFI/Plenum, New York, 1970).

18. Y. S. Touloukian, R. W. Powell, C. Y. Ho, P. G. Klemens, *Thermal Conductivity, Nonmetallic Solids,* Thermophysical Properties of Matter, vol. 2, (IFI/Plenum, New York, 1970).

19. Y. S. Touloukian, R. K. Kirby, R. E. Taylor, P. D. Desai, *Thermal Expansion Metallic Elements and Alloys,* Thermophysical Properties of Matter, vol. 12, (IFI/Plenum, New York, 1976).

20. Y. S. Touloukian, R. K. Kirby, R. E. Taylor, P. D. Desai, *Thermal Expansion, Nonmetallic Solids,* Thermophysical Properties of Matter, vol. 13, (IFI/Plenum, New York, 1976).

21. W. P. Barnes Jr., "Optical Materials - Reflective" in *Applied Optics and Engineering,* R. R. Shannon, J. C. Wyant, (Eds.), vol. VII, 97-118, (Academic Press, New York, 1979).

22. D. H. Killpatrick, "Review of the Properties of Electroless Nickel", Proceedings of the conference on Aluminum, Beryllium and Silicon Carbide Optics, Oak Ridge, W. B. Snyder, (Ed.) (Oak Ridge National Laboratory, 1993),

23. D. H. Killpatrick, "Beryllium: an Overview", Proceedings of the conference on Aluminum, Beryllium and Silicon Carbide Optics, Oak Ridge, W. B. Snyder, (Ed.) (Oak Ridge National Laboratory, 1993),

24. D. H. Killpatrick, "Properties of Materials Used for Aluminum, Beryllium and Silicon Carbide Optics", Proceedings of the conference on Aluminum, Beryllium and Silicon Carbide Optics, Oak Ridge, W. B. Snyder, (Ed.) (Oak Ridge National Laboratory, 1993).

25. R. W. Haywood, *Thermodynamic Tables in S. I. Units,* (Cambridge University Press, Cambridge, 1968).

26. W. G. Driscoll, (Ed.), Handbook of Optics, (McGraw-Hill, New York, 1978).

27. Corning Glassworks, Advanced Products Division, Corning, NY 14831, USA

28. F. Rosebury, *Handbook of Electron Tube and Vacuum Techniques*, (Addison Wesley, Reading Mass, 1965).

29. S. G. Jitendra, M. A. Pickering, R. L. Taylor, B. W. Murray, A. Lompado, "Properties of Chemical-Vapor-Deposited Silicon Carbide for Optics in Severe Environments", *Appl. Opt.*, **30**, 3166-3175 (1991).

30. M. A. Pickering, R. L. Taylor, J. T. Keeley, G. A. Graves, "Chemically Vapor Deposited Silicon Carbide (SiC) for Optical Applications" in *Space Optical Materials and Space Qualification of Optics*, R. R. Hale, (Ed.) Proc. SPIE, vol. 1118, 1-13, (SPIE, Bellingham, 1989).

31. M. A. Pickering, R. L. Taylor, J. T. Keeley, "Chemically Vapor Deposited Silicon Carbide (SiC) for Optical Applications", *Nucl. Instrum. Meth.*, **A291**, 95-100 (1990).

32. Advanced Composite Materials Corp., 1525, South Buncombe Rd, Greer, SC 29651-9208, USA

33. SCM Metal Products Inc., University Circle Research Center, 11000 Cedar Ave, Cleveland, OH 44106, USA.

34. C. J. Smithells, (Ed.) "*Metals Reference Book, 5th Edition*", (Butterworths, London, 1976).

Figure captions

1. Basic layout of a cooled mirror showing nomenclature and notation.

2. Geometry and notation of the water channels used in the analytical treatment of mirror cooling.

3. Conductive and convective thermal resistances as a function of thermal resistivity (k^{-1}) for the reference design described in Table 1 for various materials. Note that for the high conductivity materials the *convective* thermal resistance dominates and vice versa. The mirror surface temperature is also plotted and is seen to rule out certain materials such as glasses for high-power mirrors with this type of design.

4. Maximum slope errors for mirrors of the reference design (open bars) and "improved" reference design (hatched bars) as described in the text. These slopes occur at the one-sigma points of the (gaussian) incoming power distribution and correspond roughly to a "peak-to-valley" optical surface specification.

5. Principles of the cellular-pin-post cooling geometry developed by Rockwell for manufacture in silicon.

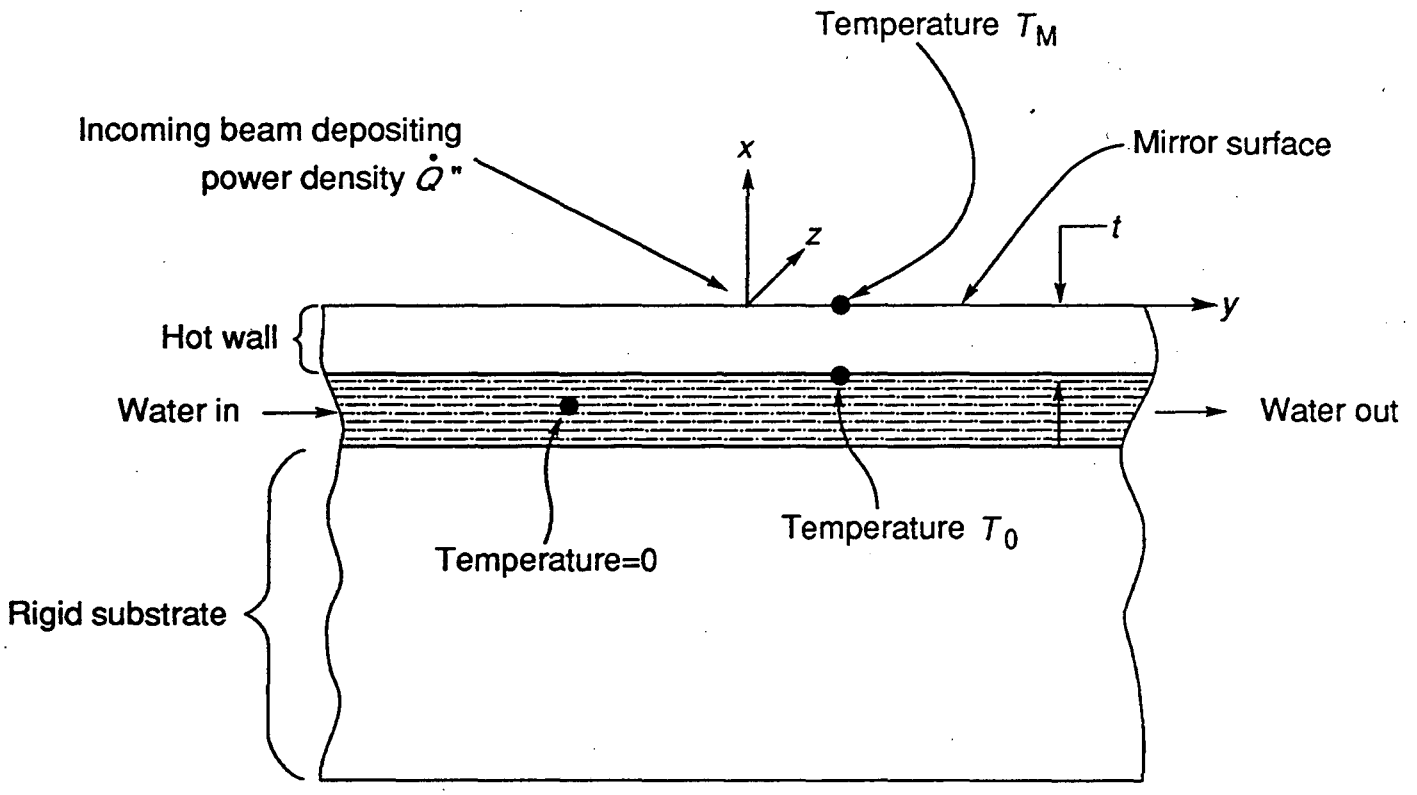

XBL 9311-4588

Fig. 1

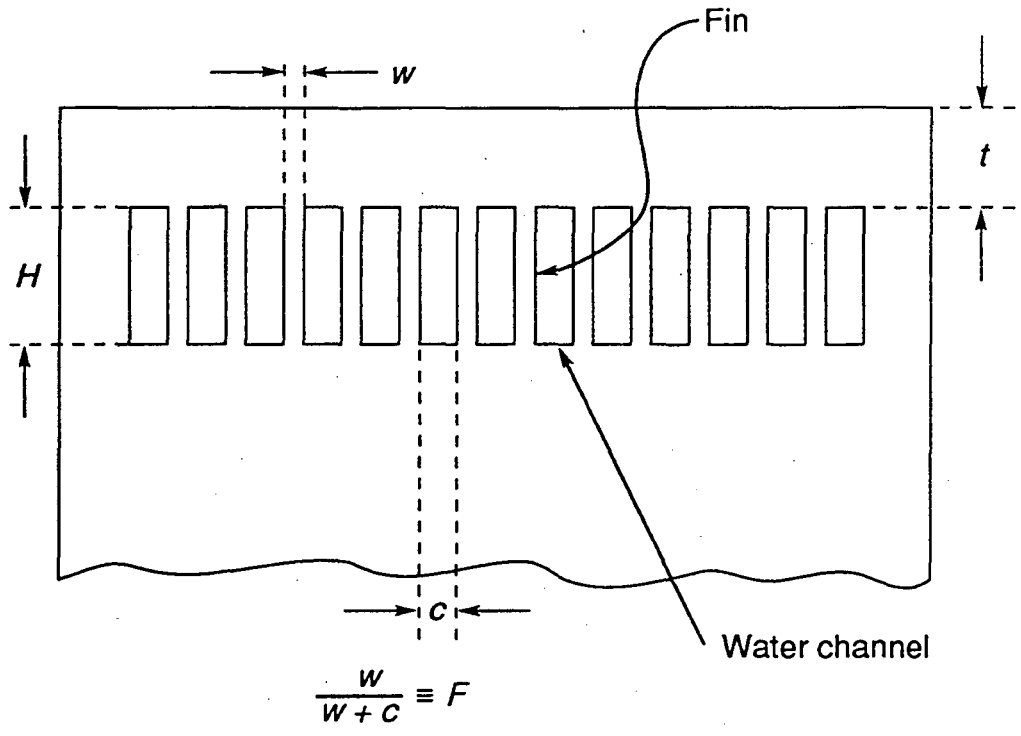

XBL 9311-4587

Fig. 2

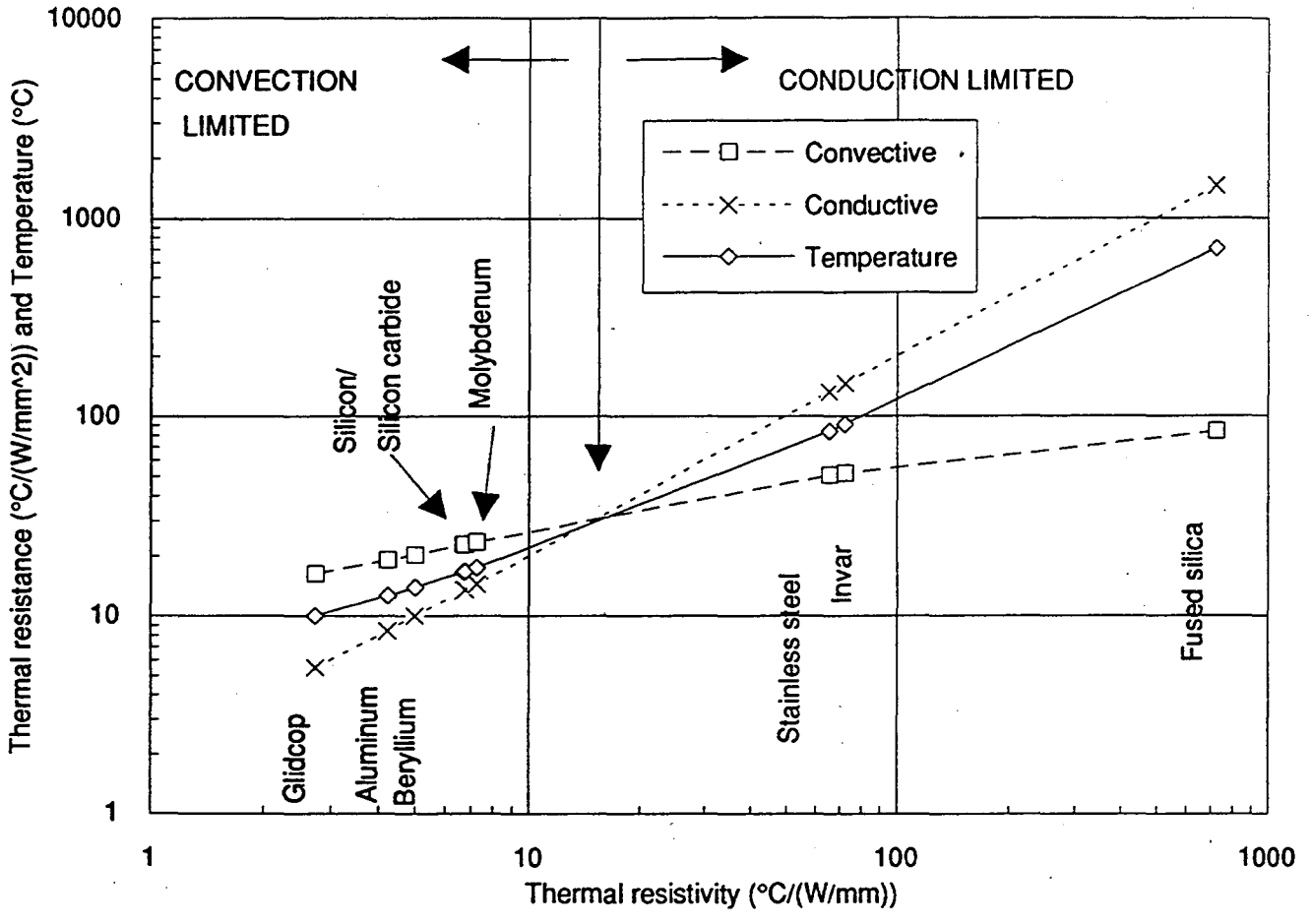
10000
1000
100
10
1
CONVECTION LIMITED
CONDUCTION LIMITED
Convective
Conductive
Temperature
Silicon/
Silicon carbide
Molybdenum
Glidcop
Aluminum
Beryllium
Stainless steel
Invar
Fused silica
Thermal resistance (°C/(W/mm^2)) and Temperature (°C)
1
10
100
1000
Thermal resistivity (°C/(W/mm))

Fig. 3

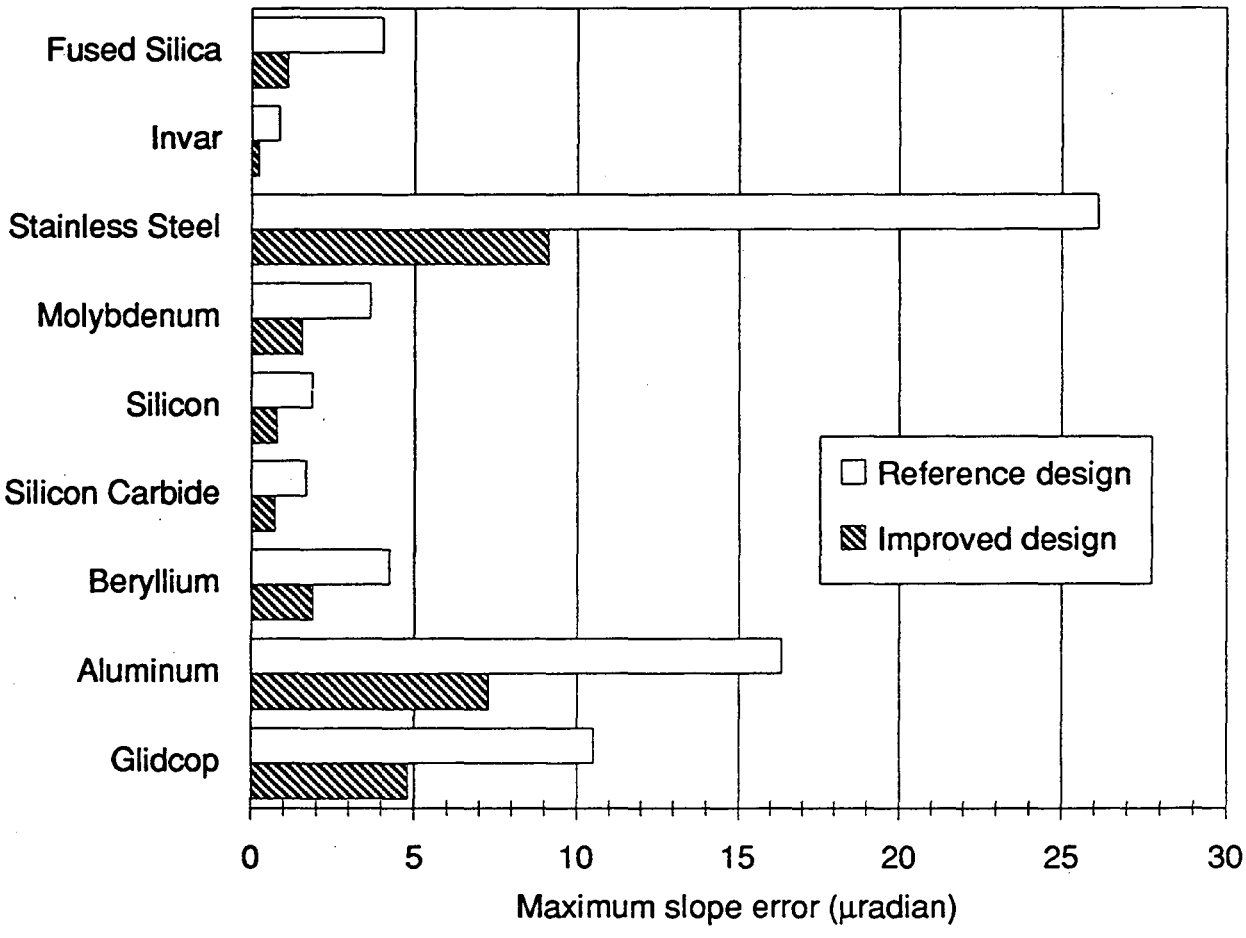
Fused Silica
Invar
Stainless Steel
Molybdenum
Silicon
Silicon Carbide
Beryllium
Aluminum
Glidcop
Reference design
Improved design
0
5
10
15
20
25
30
Maximum slope error (μradian)

Fig. 4

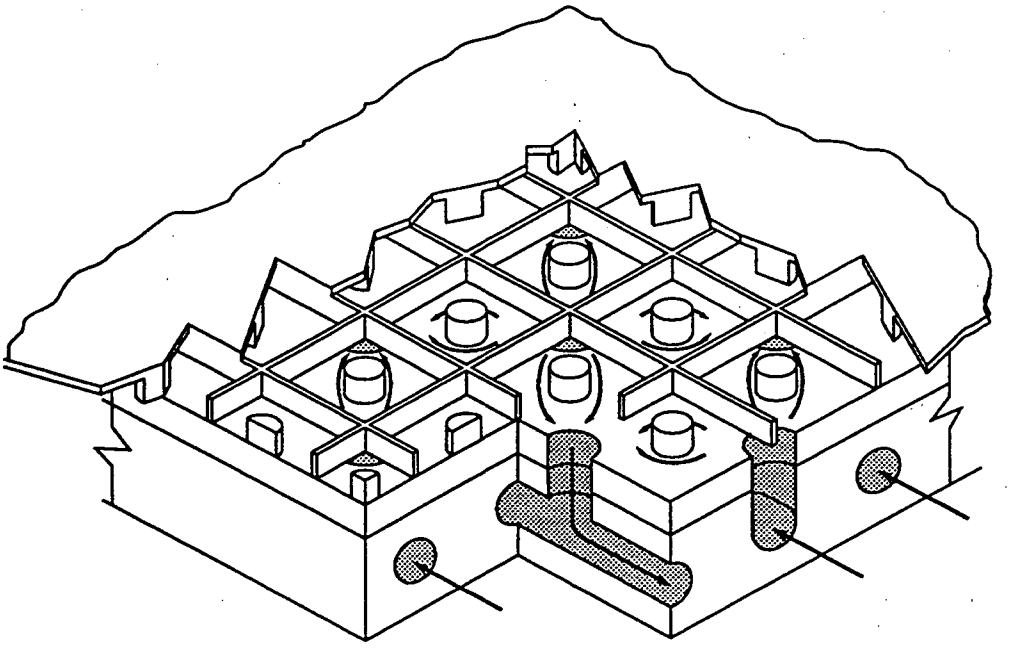

XBL 9311-4589

Fig. 5

LAWRENCE BERKELEY LABORATORY
UNIVERSITY OF CALIFORNIA
TECHNICAL INFORMATION DEPARTMENT
BERKELEY, CALIFORNIA 94720